Revision 1

Hydroxymcglassonite-(K), $KSr_4Si_8O_{20}(OH)\cdot 8H_2O$, the first Sr-bearing member of the apophyllite group, from the Wessels mine, Kalahari Manganese Field, South Africa

Hexiong Yang*[1], Xiangping Gu[2], Michael M. Scott[1]

[1]Department of Geosciences, University of Arizona, 1040 E. 4th Street, Tucson, AZ 85721-0077, USA
[2]School of Geosciences and Info-Physics, Central South University, Changsha, Hunan 410083, China

*Corresponding author: hyang@arizona.edu

Abstract

A new mineral species, hydroxymcglassonite-(K), ideally $KSr_4Si_8O_{20}(OH)\cdot 8H_2O$, has been found in the Wessels mine, Kalahari Manganese Field, Northern Cape Province, South Africa. It is granular (<0.05 mm), associated with meieranite, sugilite, aegirine, pectolite, and yuzuxiangite. The mineral is colorless, transparent with white streak and vitreous luster. It is brittle and has a Mohs hardness of 4.5-5.0; cleavage is perfect on {001} and no parting or twinning was observed. The measured and calculated densities are 2.60(3) and 2.614 g/cm^3, respectively. Optically, hydroxymcglassonite-(K) is uniaxial (+), with ω = 1.555(5), ε = 1.567(5) (white light), and absorption $O > E$. Hydroxymcglassonite-(K) is insoluble in water or hydrochloric acid. An electron microprobe analysis yielded an empirical formula (based on 13 non-H cations *pfu*) $K_{1.01}(Sr_{2.99}Ca_{1.03})_{\Sigma 4.02}Si_{7.99}O_{20}(OH)\cdot 8H_2O$, which can be simplified to $K(Sr,Ca)_4Si_8O_{20}(OH)\cdot 8H_2O$.

Hydroxymcglassonite-(K) is tetragonal with space group $P4/mnc$ and unit-cell parameters a = 9.0792(2), c = 16.1551(9) Å, V = 1331.70(9) Å^3, and Z =2. It is isostructural with hydroxyapophyllite-(K), $KCa_4Si_8O_{20}(OH)\cdot 8H_2O$, with Sr substituting for Ca. The crystal structure of hydroxymcglassonite-(K) is characterized by SiO_4

tetrahedra sharing corners to form $(Si_8O_{20})^{8-}$ sheets parallel to (001), which are connected by the K and *B* (= Sr + Ca) cations, as well as hydrogen bonding. The K cation is coordinated by eight H_2O groups and the average K–O distance of 2.941(3) Å is shorter than that of 2.950(3) – 2.975(3) Å in hydroxyapophyllite-(K) or fluorapophyllite-(K). The *B* cation is 7-coordinated (4O + $2H_2O$ + OH) and the average *B*–O distance of 2.522 (3) Å is noticeably longer than that of 2.422 – 2.435 Å in hydroxyapophyllite-(K) or fluorapophyllite-(K). The Raman spectra of hydroxymcglassonite-(K) and hydroxyapophyllite-(K) are very comparable, especially in the O-H stretching region. The discovery of hydroxymcglassonite-(K), the first Sr-bearing mineral of the apophyllite group, implies that more Sr-bearing members of the group may be found in nature or synthesized in laboratories, but the possibility for an incomplete solid solution between hydroxyapophyllite-(K) and hydroxymcglassonite-(K), due to the size difference between Sr^{2+} and Ca^{2+}, cannot be ruled out.

***Key words*:** hydroxymcglassonite-(K), apophyllite, new mineral, crystal structure, X-ray diffraction, Raman spectra

Introduction

A new mineral species, hydroxymcglassonite-(K), ideally $KSr_4Si_8O_{20}(OH)\cdot 8H_2O$, has been found in the Wessels mine, Kalahari Manganese Fields, Northern Cape Province, Republic of South Africa. It is named in honor of Mr. James (Jim) A. McGlasson, who has been interested in collecting minerals since age 10, and started field collecting after graduation from college. Jim earned his B.S. degree in geology at the New Mexico Institute of Mining and Technology and M.S. degree in geology at the Colorado School of Mines. A successful 45-year career as an exploration geologist, mine manager, and consultant has allowed him to obtain geological and mineralogical knowledge at many diverse deposits worldwide. Jim has served as the president of the

Tucson Gem and Mineral Society, and on the board of directors of the Friends of Mineralogy. With a strong belief that getting children interested in science of any kind, especially geology and mineralogy, is critical for our society and future, he has been actively and constantly involved in various educational programs for children and young students, and has donated considerable amounts of mineral specimens for their interests/hobbies. Since his retirement in 2016, Jim has been a volunteer at the University of Arizona Mineral Museum and the mineralogy laboratory of the Department of Geosciences at the University of Arizona to continue his passion for minerals while contributing his knowledge and experience to help the society and other people. The new mineral and its name have been approved by the Commission on New Minerals, Nomenclature and Classification (CNMNC) of the International Mineralogical Association (IMA 2020-066). The cotype samples have been deposited at the University of Arizona Mineral Museum (Catalogue # 22691) and the RRUFF Project (deposition # R200004), which is a part of the University of Arizona Mineral Museum.

Hydroxymcglassonite-(K) is the first Sr-bearing mineral of the apophyllite group. This paper describes its physical and chemical properties and its crystal structure determined from single-crystal X-ray diffraction data.

Sample Description and Experimental Methods

Occurrence, physical and chemical properties, and Raman spectra

Hydroxymcglassonite-(K) was found on a specimen (Fig. 1) collected from the Wessels mine, Kalahari Manganese Field, Northern Cape Province, Republic of South Africa (27° 6'51.82"S, 22°51'18.31"E). This specimen is also the type sample for meieranite (Yang et al. 2019) and yuzuxiangite (Gu et al. 2021). Hydroxymcglassonite-(K) crystals are found intergrown with isolated blue granular meieranite aggregates, which are embedded in a matrix consisting of mainly massive pale-green sugilite, along with minor prismatic grey aegirine, bladed white pectolite, and fibrous brownish

This is the peer-reviewed, final accepted version for American Mineralogist, published by the Mineralogical Society of America.
The published version is subject to change. Cite as Authors (Year) Title. American Mineralogist, in press.
DOI: https://doi.org/10.2138/am-2022-8210. http://www.minsocam.org/

yuzuxiangite (Figs 2, 3, and 4). The mineral assemblage probably formed as a result of a hydrothermal event. Conditions during metamorphism were in the range of 270-420 ºC at 0.2-1.0 kbar (Kleyenstuber 1984; Gutzmer and Beukes 1996). Detailed reviews on the geology and mineralogy of the Kalahari Manganese Field have been presented by Kleyenstuber (1984), Von Bezing *et al*. (1991), and Gutzmer & Beukes (1996).

Hydroxymcglassonite-(K) crystals are granular (< 0.05 mm). The mineral is colorless, transparent with white streak and vitreous luster. It is brittle and has a Mohs hardness of 4.5-5.0; cleavage is perfect on {010} and no twinning was observed. The density measured floatation in heavy in liquids is 2.60(3) g/cm^3 and the calculated density is 2.614 g/cm^3. Optically, hydroxymcglassonite-(K) is uniaxial (+), with ω = 1.555(5), ε = 1.567(5) (white light), and absorption $O > E$. The compatibility index based on the empirical formula is 0.031 (excellent) (Mandarino 1981). Hydroxymcglassonite-(K) is insoluble in water or hydrochloric acid.

The chemical composition of hydroxymcglassonite-(K) was determined using a Shimadzu EPMA-1720 electron microprobe (WDS mode, 15 kV, 10 nA, and a beam diameter of 5 μm). Because of the small size and vulnerability to the damage (dehydration) by the electron beam, only 5 analysis points were obtained from the single crystal used for the X-ray structure determination. As minerals in the apophyllite group commonly have the OH-F substitution, before the measurements, fluorine was particularly searched by the EDS method and then checked by the WDS scan for the $F_{K\alpha}$ peak. No F was detected by either methods with a detection limit of ~0.08 wt%. The standards used are listed in Table 1, along with the determined compositions. The resultant chemical formula, calculated on the basis of 13 non-H cations *pfu*, is $K_{1.01}(Sr_{2.99}Ca_{1.03})_{\Sigma 4.02}Si_{7.99}O_{20}(OH)\cdot 8H_2O$, which can be simplified to $K(Sr,Ca)_4Si_8O_{20}(OH)\cdot 8H_2O$. It should be pointed out that the Sr and Ca contents vary noticeably from point to point and are inversely correlated, resulting in the large standard deviations in their measurements. The crystal analyzed has Sr/(Sr+Ca)=75%. We also

This is the peer-reviewed, final accepted version for American Mineralogist, published by the Mineralogical Society of America.
The published version is subject to change. Cite as Authors (Year) Title. American Mineralogist, in press.
DOI: https://doi.org/10.2138/am-2022-8210. http://www.minsocam.org/

found another crystal with Sr/(Sr+Ca) > 80%, but its structure data are not as good as those reported here.

The Raman spectrum of hydroxymcglassonite-(K) was collected from a randomly oriented crystal on a Horiba Labram HR spectrometer in the State Key Laboratory of Powder Metallurgy, Central South University, China. The laser beam (488 nm, laser power 2 mW) was focused to 1 μm with a 100× objective on an Olympus microscope. The time of each scan in the range 100-4000 cm^{-1} was 20 minutes with a resolution of 2 cm^{-1}.

X-ray crystallography

The powder X-ray diffraction data for hydroxymcglassonite-(K) were collected on a Rigaku Xtalab Synergy single crystal diffractometer (Mo*K*α radiation) in powder mode at 50KV and 1mA (Table 2, deposited). The unit-cell parameters obtained from the powder X-ray diffraction data using the program by Holland and Redfern (1997) are: a = 9.0928 (6), c = 16.203 (2) Å, and V = 1339.65(4) $Å^3$.

Single-crystal X-ray diffraction data for hydroxymcglassonite-(K) were collected from a 0.010 x 0.002 x 0.002 mm crystal on a Rigaku Xtalab Synerg D/S 4-circle diffractometer equipped with Mo*K*α radiation. All reflections were indexed on the basis of a tetragonal unit-cell (Table 3). The systematic absences of reflections are compatible with space groups *P*4*nc* (#104) and *P*4/*mnc* (#128). The crystal structure was solved and refined using SHELX-2018 (Sheldrick 2015a, 2015b) based on space group *P*4/*mnc*, because it produced the better refinement statistics in terms of bond lengths and angles, atomic displacement parameters, and *R* factors. Difference Fourier syntheses only revealed the two H atoms (H1 and H2) associated with the H_2O group (O4), but failed to locate the H atom in the OH group (O5). This is not surprising, considering that there are only two equivalent H atoms from the OH group per unit-cell, but 16 equivalent ones for each H1 and H2. During the refinements, the structure chemistry was constrained to the

This is the peer-reviewed, final accepted version for American Mineralogist, published by the Mineralogical Society of America.
The published version is subject to change. Cite as Authors (Year) Title. American Mineralogist, in press.
DOI: https://doi.org/10.2138/am-2022-8210. http://www.minsocam.org/

empirical formula determined from the electron microprobe analysis, i.e., $K_{1.00}(Sr_{2.98}Ca_{1.02})_{\Sigma=4.00}Si_8O_{20}(OH)\cdot 8H_2O$. All non-H atoms were refined anisotropically, whereas the two H atoms (H1 and H2) were refined isotropically. Final atomic coordinates and displacement parameters for hydroxymcglassonite-(K) are given in Tables 4 and 5, respectively. Selected bond distances are presented in Table 6.

Crystal structure description and discussion

Hydroxymcglassonite-(K), ideally $KSr_4Si_8O_{20}(OH)\cdot 8H_2O$, is isostructural with hydroxyapophyllite-(K), $KCa_4Si_8O_{20}(OH)\cdot 8H_2O$ (Rouse et al. 1978) (Table 3), with Sr substituting for Ca. Its structure is characterized by SiO_4 tetrahedra sharing corners to form $(Si_8O_{20})^{8-}$ sheets parallel to (001) (Fig. 5), which are connected by the interstitial K^+ and B^{2+} (=Sr + Ca) cations and by hydrogen bonding. In the sheet, SiO_4 tetrahedra form 4- and 8-membered rings (Fig. 5). The geometry of hydrogen bonding is in accord with that in hydroxyapophyllite-(K) (Rouse et al. 1978). The bond-valence sums calculated using the parameters from Brese and O'Keeffe (1991) (Table 7) indicate that O4 is H_2O and O5 is OH.

The K^+ cation in hydroxymcglassonite-(K) is coordinated by eight H_2O groups. The average K–O distance of 2.941(3) Å (Table 6) is shorter than that of 2.950(3) – 2.975(3) Å in hydroxyapophyllite-(K) (Rouse et al. 1978) or fluorapophyllite-(K) (Chao 1971; Colville et al. 1971; Prince 1971; Pechar 1987; Ståhl et al. 1987). The *B* (= 0.74Sr + 0.26Ca) cation is 7-coordinated ($4O + 2H_2O + OH$). The average *B*–O distance of 2.522 (3) Å in hydroxymcglassonite-(K) (Table 6) is noticeably longer than that of 2.422 – 2.435 Å in hydroxyapophyllite-(K) (Rouse et al. 1978) or fluorapophyllite-(K) (Chao 1971; Colville et al. 1971; Prince 1971; Pechar 1987; Ståhl et al. 1987). This is understandable, as the *B* site is predominantly occupied by Ca^{2+} in both hydroxyapophyllite-(K) and fluorapophyllite-(K), which is significantly smaller than Sr^{2+} in ionic radius (1.06 vs. 1.21 Å) (Shannon 1976).

This is the peer-reviewed, final accepted version for American Mineralogist, published by the Mineralogical Society of America.
The published version is subject to change. Cite as Authors (Year) Title. American Mineralogist, in press.
DOI: https://doi.org/10.2138/am-2022-8210. http://www.minsocam.org/

In the ruizite-strontioruizite solid solution $(Ca,Sr)_2Mn^{3+}{}_2Si_4O_{11}(OH)_4 \cdot 2H_2O$, the *B* cation (*B* = Ca + Sr) is also 7-coordinated (Hawthorne, 1984; Fendrich et al. 2016; Yang et al. 2021) and the average *B*-O bond distance increases linearly with increasing X = Sr/(Sr + Ca), following the equation $<B\text{-O}> = 0.1468X + 2.4475$ (Å) ($R^2 = 0.98$) (Yang et al. 2021). With Sr = 0.74 for hydroxymcglassonite-(K), we obtain $<B\text{-O}> = 2.556$ Å, which is slightly longer than our measured value of 2.522 Å.

The Raman spectrum of hydroxymcglassonite-(K) is plotted in Figure 6. Based on previous Raman spectroscopic studies on both hydroxyapophyllite-(K) and fluorapophyllite-(K) (Adams et al. 1980; Sidorov 2000; Frost and Xi 2012; Goryainov et al. 2012; Ogorodova et al. 2019), we made the tentative assignments of major Raman bands for hydroxymcglassonite-(K) (Table 8). For comparison, the Raman spectra of hydroxyapophyllite-(K) (http://rruff.info/R050169) and fluorapophyllite-(K) (http://rruff.info/R050021) from the RRUFF Project were also plotted in Figure 6. The similarities among the three spectra are evident. The difference in peak intensities among the spectra principally results from the different crystal orientations when the data were collected.

According to Frost and Xi (2012), Goryainov et al. (2012), and Ogorodova et al. (2019), the key difference between the Raman spectra of hydroxyapophyllite-(K) and fluorapophyllite-(K) is the observation of two Raman bands in the O-H stretching region at ~3565 (due to the O-H stretching vibrations in H_2O) and 3625 cm^{-1} (due to the O-H stretching vibrations in OH) for the former and only one band at ~3565 cm^{-1} for the latter. The observation of the Raman peak at ~3625 cm^{-1} is regarded as a distinctive diagnostic feature indicating the presence of the OH group in the apophyllite-type structures (Ogorodova et al. 2019). The Raman spectrum of hydroxymcglassonite-(K) exhibits two major bands in the O-H stretching vibration region, consistent with that of hydroxyapophyllite-(K), indicating the presence of both H_2O and OH groups in its structure.

Implications

Apophyllite-type minerals are of great industrial and technological interest because they are examples of naturally occurring single-sheet silicates and their reactions with chlorosilanes yield apophyllite-based organosilicate polymers on both sides of silicate sheets, which possess a unique combination of hydrophobic and hydrophilic properties that are highly tunable (Chao et al., 2001; Chen et al., 2007; Specht et al., 2010). According to the IMA-CNMNC guidelines for mineral nomenclature (Hatert et al. 2013), minerals of the apophyllite group are named based on the chemical formula $A^{+}Ca_4Si_8O_{20}X^{-}\cdot 8H_2O$, where A^{+} (= K, Na, Cs, or NH_4) and X^{-} (= F or OH) are used as suffixes and prefixes (fluor for F and hydroxy for OH), respectively, in the naming. To date, there are five members in the apophyllite group: fluorapophyllite-(K), fluorapophyllite-(Na), fluorapophyllite-(NH_4), fluorapophyllite-(Cs), and hydroxyapophyllite-(K). The discovery of hydroxymcglassonite-(K), the first Sr-bearing member of the apophyllite group, suggests that more Sr-dominant members of the group may be found in nature or synthesized in laboratories. For naturally occurring Sr-dominant members, the same naming guidelines with *A* and *X* as suffixes and prefixes, respectively, should be employed.

The Sr^{2+}-Ca^{2+} substitution in various minerals and materials has been a subject of numerous investigations owing to its effects on the properties of luminescent materials (e.g., Yu et al., 2012; Misevicius et al. 2019; Wang et al. 2020), bioactive glasses (e.g., Martin et al. 2012; Pedone et al. 2021), and solid solutions (e.g., Gottschalk et al. 1998; Ellemann-Olesen and Malcherek 2005). In some cases, the Sr^{2+}-Ca^{2+} substitution may result in incomplete solid solutions due to the difference in the Ca^{2+} and Sr^{2+} ionic radii (r = 1.06 Å for 7-coordinated Ca^{2+} and 1.21 Å for Sr^{2+}) (Shannon 1976). There are two kinds of incomplete solid solutions. One of them is that the two endmembers assume different structure symmetries, such as $CaCO_3$ (*R*-3*c* calcite) vs. $SrCO_3$ (*Pmcn*

strontianite) or $CaSO_4$ (*Bmmb* anhydrite) vs. $SrSO_4$ (*Pnma* celestine). The other kind is that the two endmembers possess the same symmetry, but it is different from that for the intermediate phases, as a consequence of the Ca^{2+} and Sr^{2+} ordering into different crystallographic sites. For example, in the system of $Ca_2Mn^{3+}{}_2Si_4O_{11}(OH)_4 \cdot 2H_2O$ (ruizite) --- $Sr_2Mn^{3+}{}_2Si_4O_{11}(OH)_4 \cdot 2H_2O$ (strontioruizite), the two endmembers have the same *C*2 symmetry, but the intermediate phase with the Ca:Sr ≅ 1:1, ideally $SrCaMn^{3+}{}_2Si_4O_{11}(OH)_4 \cdot 2H_2O$ (taniajacoite), exhibits the *C*-1 symmetry due to the preferential occupation of Sr^{2+} and Ca^{2+} over two distinct, 7-coordinated sites (Yang et al. 2021). Since both hydroxyapophyllite-(K), $KCa_4Si_8O_{20}(OH) \cdot 8H_2O$, and hydroxymcglassonite-(K), $KSr_4Si_8O_{20}(OH) \cdot 8H_2O$, have the same symmetry *P*4*/mnc*, it then begs the question whether the intermediate phase, $K(Sr_2Ca_2)Si_8O_{20}(OH) \cdot 8H_2O$, possesses the same symmetry as the two endmembers. In other words, could Sr^{2+} and Ca^{2+} in the intermediate phase be ordered into two distinct sites, as in taniajacoite, thus resulting in a reduction in the structure symmetry? Interestingly, Matsueda et al. (1981) reported that fluorapophyllite-(Na), $NaCa_4Si_8O_{20}F \cdot 8H_2O$, exhibits the orthorhombic symmetry *Pnnm*, rather than the tetragonal symmetry *P*4*/mnc* as for fluorapophyllite-(K). They ascribed this symmetry reduction to the silicate-sheet distortion caused by the substitution of small Na^+ for large K^+. As a consequence, the 8-fold position (8*h* with the site symmetry *m*) occupied by Ca^{2+} in the *P*4*/mnc* structure splits into two 4-fold positions (4*g* with the site symmetry *m*), Ca1 and Ca2, in the *Pnnm* structure. An examination of the fluorapophyllite-(Na) structure (Matsueda et al. 1981) reveals that, although both Ca1 and Ca2 sites are still 7-coordinated, as in fluorapophyllite-(K), the Ca1 site is significantly larger than the Ca2 site, with <Ca1-(O,F)> = 2.426 Å vs. <Ca2-(O,F)> =2.367 Å. This observation suggests that the apophyllite-type structure is intrinsically capable of assuming an ordered orthorhombic *Pnnm* structure with the Ca1 and Ca2 sites occupied by two different B^{2+} cations. Thus, we cannot rule out the possibility that the intermediate phase between hydroxyapophyllite-(K) and

hydroxymcglassonite-(K) could possess an ordered structure with large Sr^{2+} and small Ca^{2+} occupying two distinct sites, such as the Ca1 and Ca2 sites in fluorapophyllite-(Na) (Matsueda et al. 1981).

Acknowledgements

We are grateful for the constructive comments by Anthony R. Kampf and Radek Å. Koda.

References Cited

Adams, D.M., Armstrong, R.S., and Best, S.P. (1980) Single-crystal Raman spectroscopic study of apophyllite, a layer silicate. Inorganic Chemistry, 20, 1771-1776.

Brese, N.E. and O'Keeffe, M. (1991) Bond-valence parameters for solids. Acta Crystallographica B47, 192–197.

Burke E A J (2008) Tidying up mineral names: an IMA-CNMNC scheme for suffixes, hyphens and diacritical marks. The Mineralogical Record, 39, 131-135.

Chen, C., Yebassa, D., and Raghavan, D. (2007) Synthesis, characterization, and Mechanical properties evaluation of thermally stable apophyllite vinyl ester nanocomposites. Polymers for Advanced Technologies, 18, 574–581.

Chao, G.Y. (1971) The refinement of the crystal structure of apophyllite. II. Determination of the hydrogen positions by X-ray diffraction. American Mineralogist, 56, 1234–1242.

Chao, T.C., Katsoulis, D.E., and Kenney, M.E. (2001) Synthesis and characterization of organosilicon sheet and tube polymers. Chemistry of Materials, 13, 4269–4277.

Colville, A.A., Anderson, C.P., and Black, P.M. (1971) Refinement of the crystal structure of apophyllite. I. X-ray diffraction and physical properties. American Mineralogist, 56, 1222-1233.

Dunn, P.J., Rouse, R.C., Norberg, J.A., and Peacor, D.R. (1978) Hydroxyapophyllite, a new mineral, and a redefinition of the apophyllite group I. Description,

occurrences, and nomenclature II. Crystal structure. American Mineralogist, 63, 196-202.

Ellemann-Olesen, R. and Malcherek, T. (2005) The structure of $SrTiOGeO_4$ and its solid solution with $CaTiOGeO_4$. Physics and Chemistry of Minerals, 32, 531-545.

Fendrich, K.V., Downs, R.T., and Origlieri, M.J. (2016) Redetermination of ruizite, $Ca_2Mn^{3+}_2[Si_4O_{11}(OH)](OH)_2 \cdot 2H_2O$. Acta Crystallographica, E72, 959-963.

Frost, R.L. and Xi, Y. (2012) Raman spectroscopic study of the minerals apophyllite-(KF) $KCa_4Si_8O_{20}F \cdot 8H_2O$ and apophyllite-(KOH) $KCa_4Si_8O_{20}(F,OH) \cdot 8H_2O$. Journal of Molecular Structure, 1028, 200–207.

Goryainov, S.V., Krylov, A.S., Pan, Y., Madyukov, I.A., Smirnove, M.B., and Vtyurind, A.N. (2012) Raman investigation of hydrostatic and nonhydrostatic compressions of OH- and F-apophyllites up to 8 GPa. Journal of Raman Spectroscopy, 43, 439–447.

Gottschalk, M., Najorka, J., and Andrut, M. (1998) Structural and compositional characterization of synthetic (Ca,Sr)-tremolite and (Ca,Sr)-diopside solid solutions. Physics and Chemistry of Minerals, 25, 415-428.

Gu, X., Yang, H., and Xie, X. (2021) Yuzuxiangite, IMA 2020-084, in: CNMNC Newsletter 60, European Journal Mineralogy, 33, https://doi.org/10.5194/ejm-33-203-2021.

Gutzmer, J. and Beukes, N.J. (1996) Mineral paragenesis of the Kalahari manganese field, South Africa. Ore Geology Reviews, 11, 405-428.

Hatert, F., Mills, S.J., Pasero, M., and Williams, P.A. (2013) CNMNC guidelines for the use of suffixes and prefixes in mineral nomenclature, and for the preservation of historical names. European Journal of Mineralogy, 25, 113-115.

Hawthorne, F.C. (1984) The crystal structure of ruizite, a sorosilicate with an $[Si_4O_{13}]$ cluster. Tschermaks Mineralogische und Petrographische Mitteilungen, 33, 135-146.

Holland, T.J.B. and Redfern, S.A.T. (1997) Unit cell refinement from powder diffraction data: the use of regression diagnostics. Mineralogical Magazine, 61, 65-77.

Kleyenstuber, A.S.E. (1984) The mineralogy of the manganese bearing Hotazel formation of the Proterozoic Travsvaal sequence of Griqualand West, South Africa. Transaction of Geological Society of South Africa, 87, 267-275.

Mandarino, J.A. (1981) The Gladstone-Dale relationship: Part IV. The compatibility concept and its application. Canadian Mineralogist 19, 441-450.

Martin, R.A., Twyman, H.L., Rees, G.J., Barney, E.R., R. M. Moss, R.M., J. M. Smith, J.M., Hill, R.G., Cibin, G., Charpentier, T., Smith, M.E., Hanna, J.V. and Newport, R.J. (2012) An examination of the calcium and strontium site distribution in bioactive glasses through isomorphic neutron diffraction, X-ray diffraction, EXAFS and multinuclear solid state NMR. Journal of Materials Chemistry, 22, 22212-22223.

Matsueda, H., Miura, Y., Rucklidge, J., and Kato, T. (1981) Natroapophyllite, a new orthorhombic sodium analog of apophyllite. American Mineralogist, 66, 410-423.

Misevicius, M., Jonikavicius, K., Jørgensen, J.-E., and Balevicius, V. (2019) Effect of partial substitution of Ca for Sr on crystal structure and luminescence of Ce-doped $Sr_4Al_{14}O_{25}$. Journal of Solid State Chemistry, 274, 116-123.

Ogorodova, L.P., Melchakova, L.V., M. Vigasina, M.F., Gritsenko, Yu. G., Ksenofontov, D.A., and Bryzgalov, I.A. (2019) Thermodynamic Properties of Fluorapophyllite-(K) and Hydroxyapophyllite-(K). Geochemistry International, 57, 805–811.

Pechar, F. (1987) An X-ray Diffraction Refinement of the Crystal Structure of Natural Apophyllite. Crystal Research & Technology, 22, 1041-1046.

Pedone, A., Cannillo, V., Menziani, M.C. (2021) Toward the understanding of crystallization, mechanical properties and reactivity of multicomponent bioactive glasses. Acta Materialia, 213, 116977 (1-15).

Prince, E. (1971) Refinement of the crystal structure of apophyllite. III. Determination of the hydrogen positions by neutron diffraction. American Mineralogist, 56, 1241-1251.

Rouse, R.C., Peacor, D.R., and Dunn, P.J. (1978) Hydroxyapophyllite, a new mineral, and a redefinition of the apophyllite group II. Crystal structure. American Mineralogist, 63, 196-202.

Shannon, R.D. (1976) Revised effective ionic radii and systematic studies of interatomic distances in halides and chalcogenides. Acta Crystallographica, A32, 751–767.

Sheldrick, G.M. (2015a) SHELXT – Integrated space-group and crystal structure determination. Acta Crystallographica A71, 3-8.

Sheldrick, G.M. (2015b) Crystal structure refinement with SHELX. Acta Crystallographica, C71, 3-8.

Sidorov, T.A. (2000) The molecular structure and vibrational spectrum of apophyllite, $KCa_4(Si_4O_{10})_2(F,OH)\cdot 8H_2O$. Russian Journal of Physical Chemistry, 74, 377-381.

346 Specht, K.M., Jackson, M., Sunkel, B. and Boucher, M.A. (2010) Synthesis of a
347 functianalized sheet silicate derived from apophyllite and further modification by
348 hydrosilylation. Applied Clay Science, 47, 212–215.

349 Ståhl, K., Kvick, Å., and Ghose, S. (1987) A neutron diffraction and thermogravimetric
350 study of the hydrogen bonding and dehydration behaviour in fluorapophyllite,
351 $KCa_4(Si_8O_{20})F{\cdot}8H_2O$, and its partially dehydrated form. Acta Crystallographica,
352 B43, 517–523.

353 Von Bezing, K.L., Dixon, R.D., Pohl, D., and Cavallo, G. (1991) The Kalahari
354 Manganese Field, an update. Mineralogical Record, 22, 279-297.

355 Wang, Q.-Y., Yuan, P., Wang, T.-W., Yin, Z.-Q., and Lu, F.-C. (2020) Effect of Sr and
356 Ca substitution of Ba on the photoluminescence properties of the Eu^{2+} activated
357 $Ba_2MgSi_2O_7$ phosphor. Ceramics International, 46, 1374-1382.

358 Yang, H., Gu, X., Downs. R.T., Evans, S.H., Van Nieuwenhuizen, J.J., Lavinsky, R.M.,
359 Xie, X. (2019) Meieranite, $Na_2Sr_3MgSi_6O_{17}$, a new mineral from the Wessels
360 mine, Kalahari Manganese Fields, South Africa. The Canadian Mineralogist, 57,
361 457-466.

362 Yang, H., Gu, X., Cairncross, B., Downs, R.T., and Evans, S.H., (2021) Taniajacoite and
363 strontioruizite, two new minerals isostructural with ruizite, from the N'Chwaning
364 III mine, Kalahari Manganese Field, South Africa. Canadian Mineralogist (in
365 press: https://doi.org/10.3749/canmin.2000037)

366 Yu, J., Zhang, X., Hao, Z., Luo, Y., Wang, X., and Zhang, J. (2012) Blue emission of
367 $Sr_{2-x}Ca_xP_2O_7{:}Eu^{2+}$ for near UV excitation. Journal of Alloys and Compounds,
368 515, 39-43.

369

370

371

372

373

374

375

376

377

List of Figure Captions

Figure 1. The specimen on which colorless hydroxymcglassonite-(K) crystals are found in intergrowth with isolated blue granular meieranite aggregates, which are embedded in a matrix consisting of mainly massive pale-green sugilite, along with minor prismatic grey aegirine, bladed white pectolite, and brownish fibrous yuzuxiangite.

Figure 2. A microscopic view of colorless hydroxymcglassonite-(K) intergrown with blue granular meieranite.

Figure 3. A photomicrograph showing the occurrence and association of hydroxymcglassonite-(K) (reflected light, parallel nicols).

Figure 4. Backscattered electron image of hydroxymcglassonite-(K), associated with meieranite and sugilite.

Figure 5. Raman spectra of hydroxymcglassonite-(K), hydroxyapophyllite-(K), and fluorapophyllite-(K).

Figure 6. Crystal structure of hydroxymcglassonite-(K). SiO_4 tetrahedra and Sr-dominant polyhedra are green and yellow, respectively. The K, O4 (H_2O), O5 (OH), and H atoms are shown as large purple, medium aqua, medium red, and small blue spheres, respectively. Thin black lines show the unit cell.

List of Tables

Table 1. Chemical composition of hydroxymcglassonite-(K).

Table 2. Powder X-ray diffraction data for hydroxymcglassonite-(K).

Table 3. Summary of crystallographic data and refinement results for hydroxymcglassonite-(K).

Table 4. Fractional atomic coordinates and isotropic or equivalent isotropic displacement parameters ($Å^2$) for hydroxymcglassonite-(K).

Table 5. Atomic displacement parameters ($Å^2$) for hydroxymcglassonite-(K).

Table 6. Selected bond distances (Å) in hydroxymcglassonite-(K).

Table 7. Bond-valence sums for hydroxymcglassonite-(K).

Table 8. Tentative assignments of major Raman bands for hydroxymcglassonite-(K).

Table 1. Electron microprobe analysis data (in wt.%) for hydroxymcglassonite-(K).

Constituent	Mean	Range	Stand. Dev.	Probe Standard
SiO_2	45.99	44.94-47.27	0.99	SiO_2
K_2O	4.56	4.17-5.93	0.32	$KAlSi_3O_8$
CaO	5.52	3.06-7.21	2.19	$CaSiO_3$
SrO	29.66	26.36-33.67	3.11	$SrSO_4$
H_2O*	14.67			
Total	100.40	100.05-100.78	0.28	

Note: *Calculated based on the structure.

Table 3. Comparison of mineralogical data for hydroxyapophyllite-(K) and Hydroxymcglassonite-(K)

	hydroxyapophyllite-(K)	Hydroxymcglassonite-(K)
Ideal chemical formula	$KCa_4Si_8O_{20}(OH,F)\cdot 8H_2O$	$KSr_4Si_8O_{20}(OH)\cdot 8H_2O$
Crystal symmetry	Tetragonal	Tetragonal
Space group	*P*4/*mnc*	*P*4/*mnc*
a (Å)	8.979(4)	9.0792(2)
c (Å)	15.83(1)	16.1551(9)
V (Å^3)	1276.253	1331.70(10)
Z	2	2
ρ_{obs}, ρ_{cal} (g/cm^3)	2.37, 2.36	2.59, 2.60
Optical properties	uniaxial (+)	uniaxial (+)
ω	1.52	1.555
ε	1.53	1.567
2θ range for data collection	≤54.77	≤67.31
No. of reflections collected	1049	10474
No. of independent reflections	757	1262
No. of reflections with $I > 2\sigma(I)$	696	1046
No. of parameters refined		61
R(int)		0.039
Final R_1, wR_2 factors [$I > 2\sigma(I)$]	0.035, 0.038	0.040, 0.088
Goodness-of-fit		1.069
Reference	Rouse et al. (1978)	This study

Table 6. Selected bond distances (Å) for hydroxymcglassonite-(K) and hydroxyapophyllite-(K).

	Hydroxymcglassonite-(K)	Hydroxyapophyllite-(K)
K—O4 × 8	2.941(3)	2.954(3)
B—O3 × 2	2.487(2)	2.403(2)
—O3 × 2	2.509(2)	2.416(2)
—O5	2.5497(5)	2.435(1)
—O4 × 2	2.555(3)	2.486(3)
Ave.	2.522	2.435
Si—O3	1.590(2)	1.584(3)
—O1	1.6185(11)	1.622(3)
—O2	1.629(2)	1.617(2)
—O2	1.636(2)	1.644(2)
Ave.	1.619	1.616

Table 7. Bond-valence sums for hydroxymcglassonite-(K).

	K	*B*	Si	Sum
O1			1.015x2→	2.029
O2			0.984	1.953
			0.969	
O3		0.337 x2↓	1.100	1.754
		0.317 x2↓		
O4	0.112 x 8↓	0.280 x2↓		0.392
O5		0.237 x 4→		0.948
Sum	0.896	2.105	4.068	

Note: The bond valence sum for *B* was calculated based on ($0.74Sr^{2+}$ + $0.26Ca^{2+}$).

Table 8. Tentative assignments of major Raman bands for hydroxymcglassonite-(K).

Bands (cm^{-1})	Assignment
3621	O-H stretching vibration in OH groups
3572	O-H stretching vibration in H_2O groups
940-1060	Si-O stretching vibrations in SiO_4 units
772, 861	H_2O libration
662, 635	Si-O-Si bending vibrations
430, 574	O-Si-O bending vibrations
160-321	Lattice modes and *B*-O interaction vibrations

Note: $B = Sr^{2+} + Ca^{2+}$.

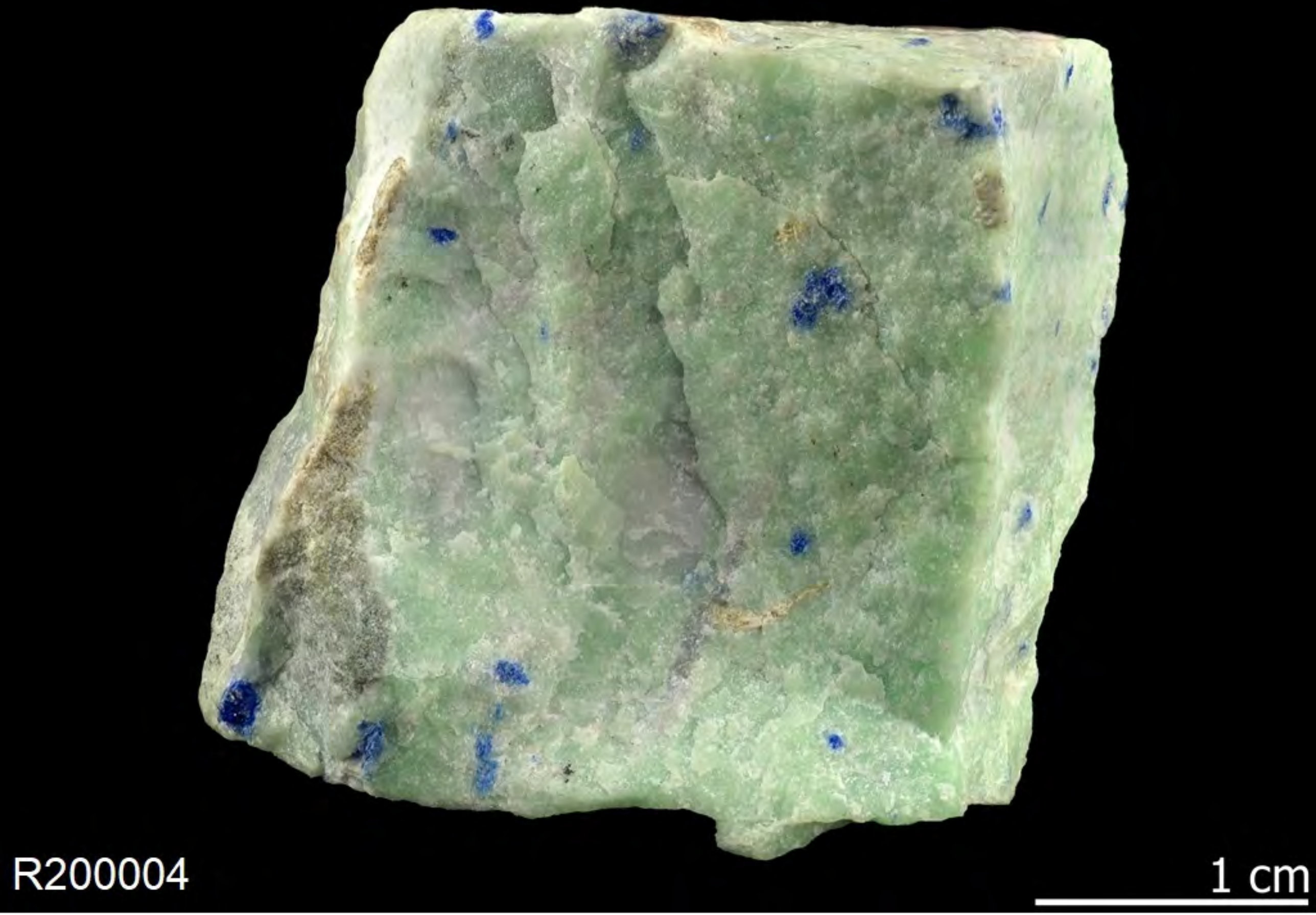

Figure 1

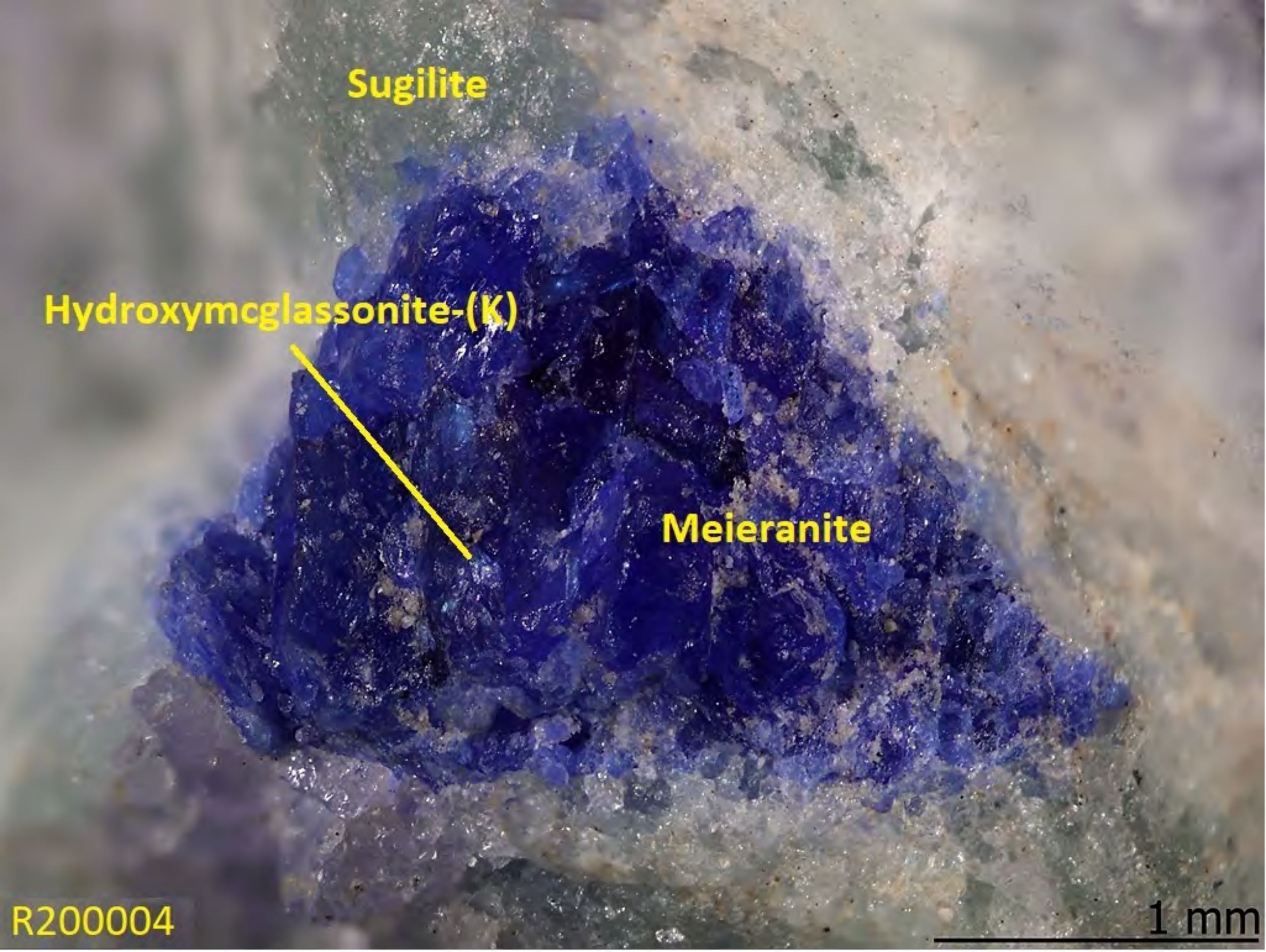

Figure 2.

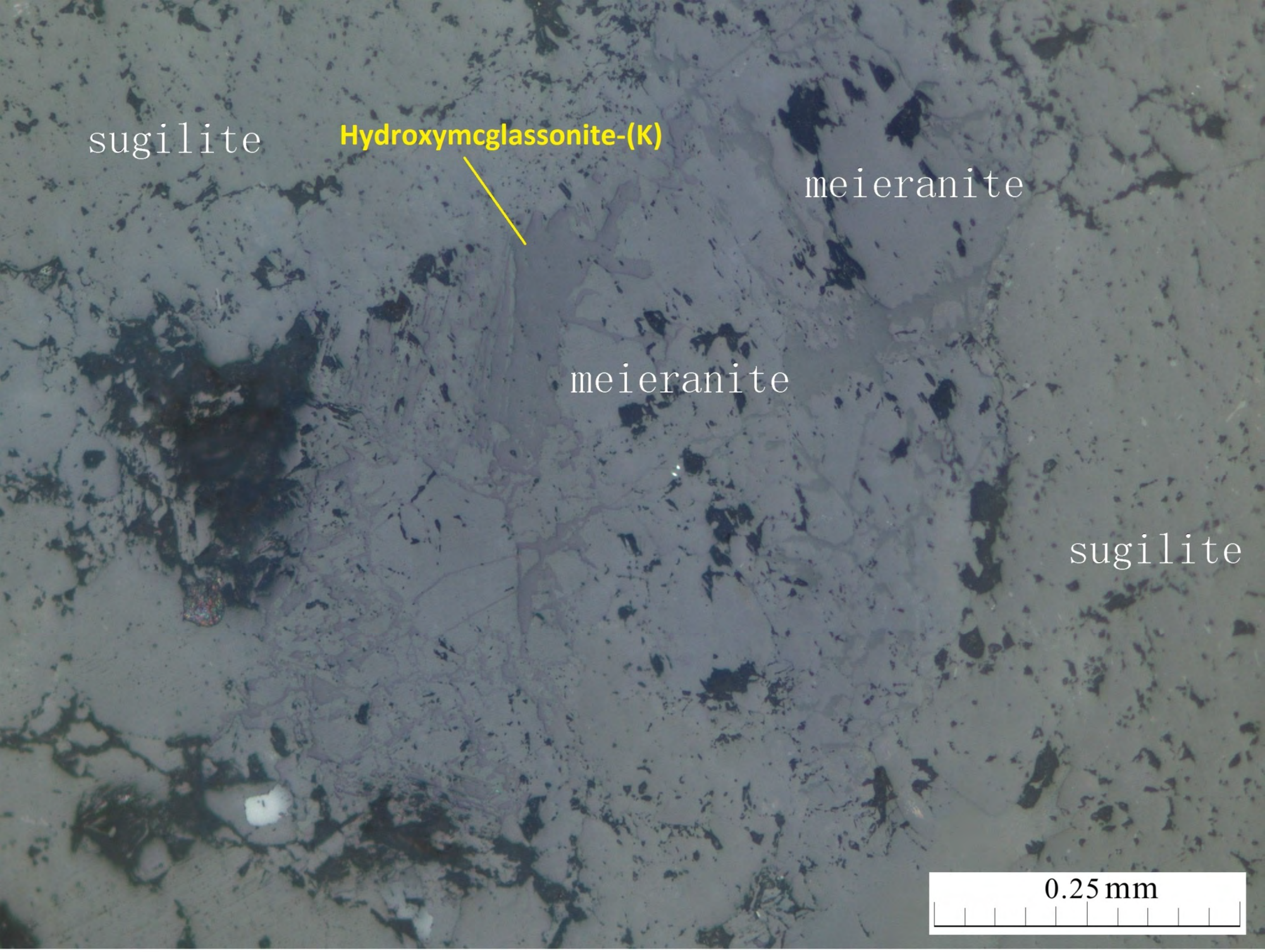
sugilite
Hydroxymcglassonite-(K)
meieranite
meieranite
sugilite
0.25 mm

Figure 3.

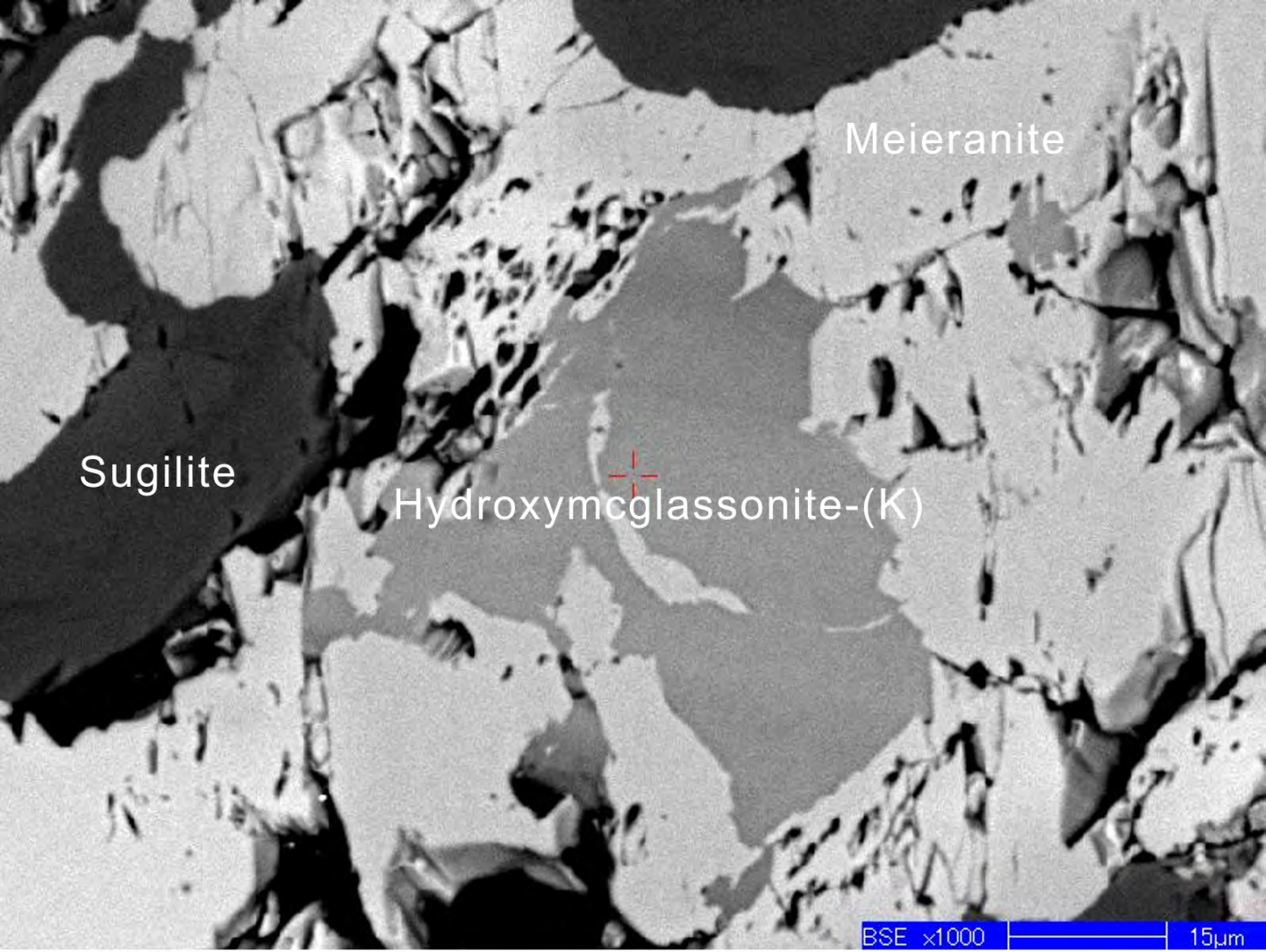
Meieranite
Sugilite
Hydroxymcglassonite-(K)
BSE x1000
15µm

Figure 4.

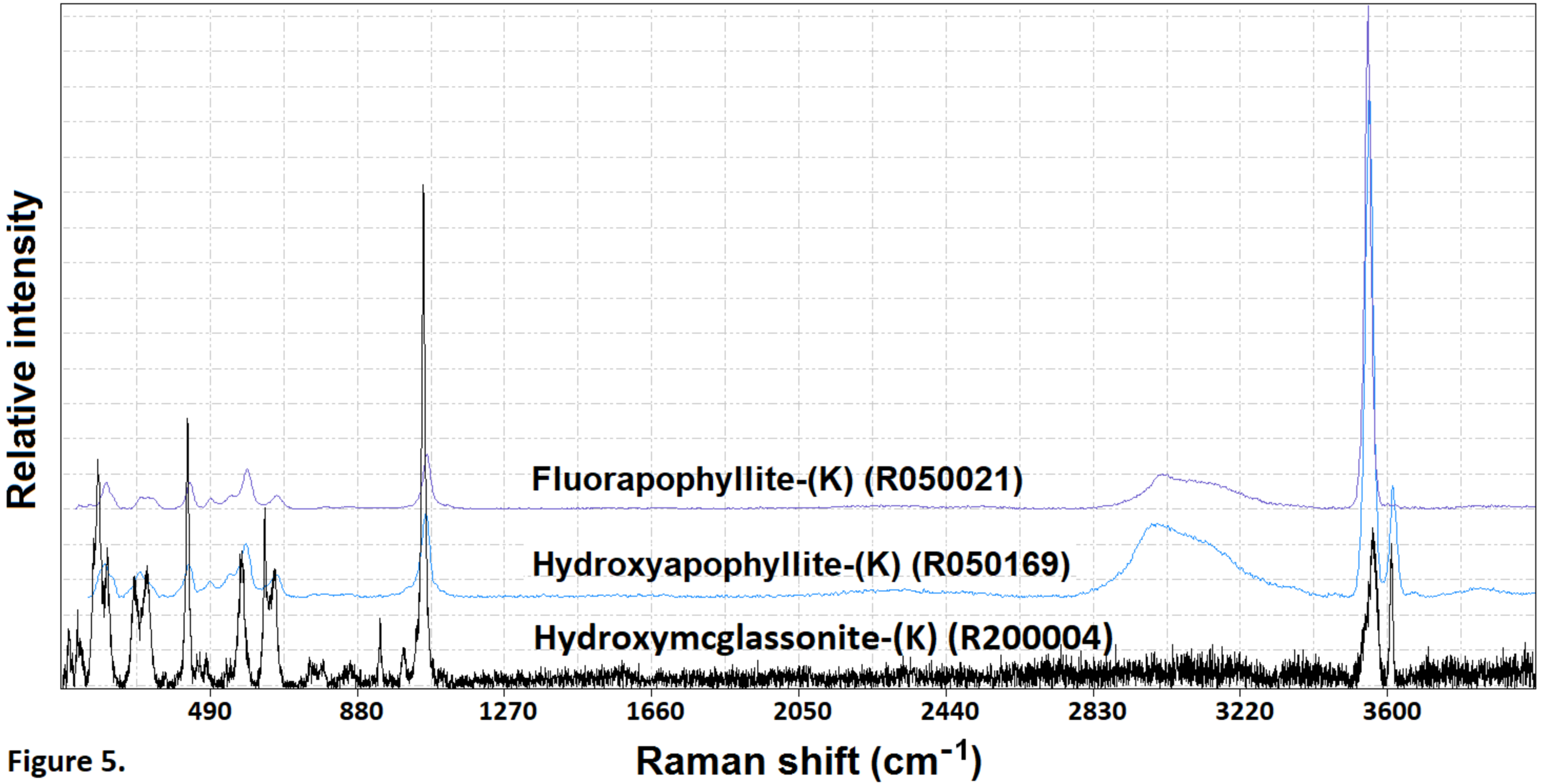
Relative intensity
Fluorapophyllite-(K) (R050021)
Hydroxyapophyllite-(K) (R050169)
Hydroxymcglassonite-(K) (R200004)
490
880
1270
1660
2050
2440
2830
3220
3600
Raman shift (cm-1)

Figure 5.

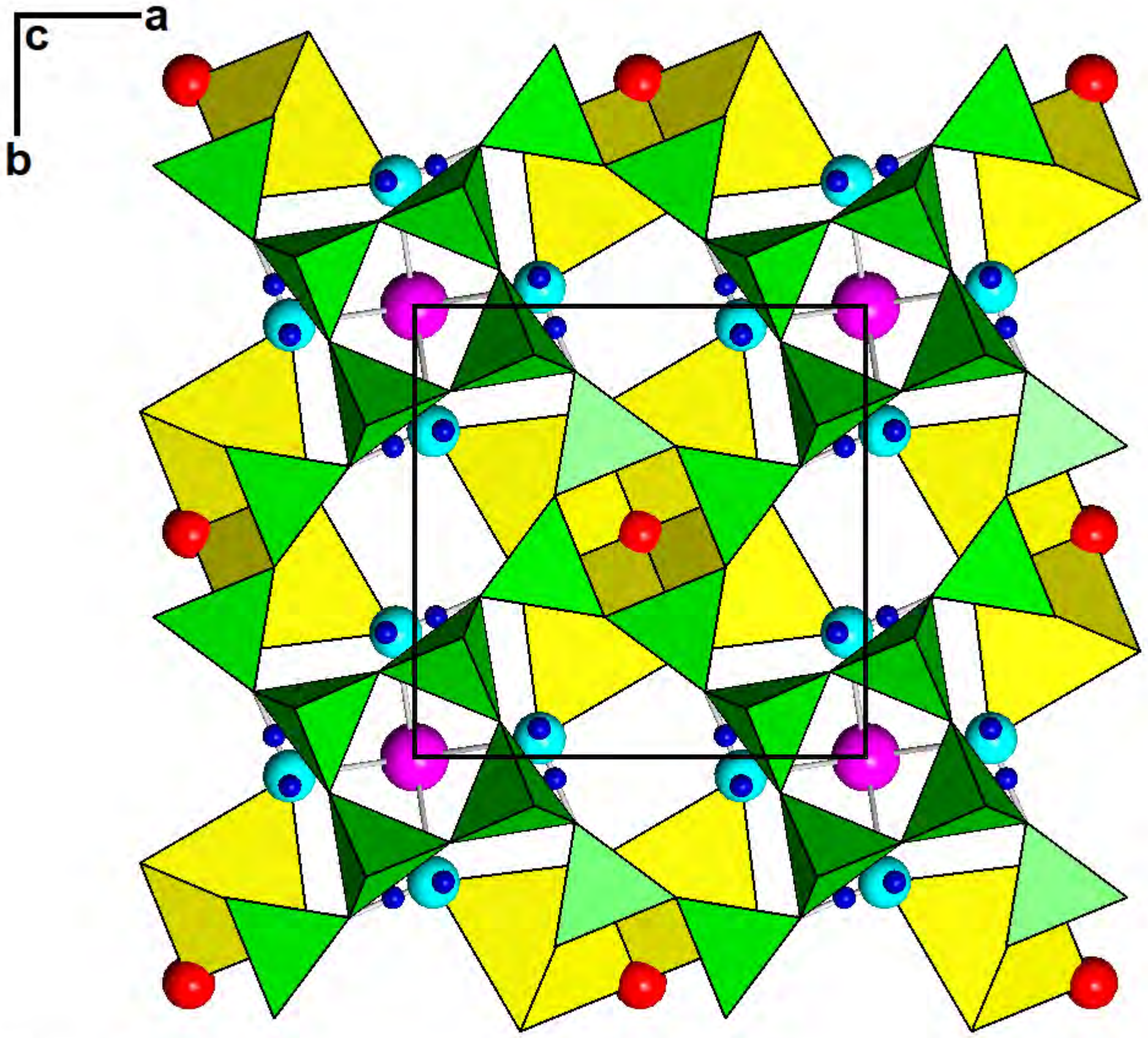

Figure 6.